X-RAY HIGH RESOLUTION AND IMAGING SPECTROSCOPY OF SUPERNOVA REMNANTS

Jacco Vink

Astronomical Institute, University Utrecht, PO Box 80000, NL-3508TA, Utrecht, The Netherlands

ABSTRACT

The launch of Chandra and XMM-Newton has led to important new findings concerning the X-ray emission from supernova remnants. These findings are a result of the high spatial resolution with which imaging spectroscopy is now possible, but also some useful results have come out of the grating spectrometers of both X-ray observatories, despite the extended nature of supernova remnants. The findings discussed here are the evidence for slow equilibration of electron and ion temperatures near fast supernova remnant shocks, the magnetic field amplification near remnant shocks due to cosmic ray acceleration, a result that has come out of studying narrow filaments of X-ray synchrotron emission, and finally the recent findings concerning Fe-rich ejecta in Type Ia remnants and the presence of a jet/counter jet system in the Type Ib supernova remnant Cas A.

Key words: Supernova remnants; shocks; cosmic rays;X-rays.

1. INTRODUCTION

Supernovae are the most important sources of kinetic energy and chemical enrichment of galaxies. By studying supernova remnants (SNRs) we hope to learn about supernova explosion properties and chemical yields. Moreover, because of their energy and large extent, SNRs are thought to be the principal sources of cosmic rays of energies up to $\sim 10^{15}$ eV. Note that the large sizes of SNRs are also an important ingredient for their ability to accelerate cosmic rays, because astrophysical sources cannot accelerate particles beyond energies for which their gyro-radii are larger than the sources themselves. This means that for cosmic ray acceleration high magnetic fields and/or large objects sizes are required.

Their large sizes, several parsecs, make SNRs also rewarding targets for X-ray imaging spectroscopy. X-ray imaging spectroscopy made a great leap forward with the launch of the *Chandra* and *XMM-Newton* satellites. It is now possible to obtain spectra with a spectral resolution of $E/\Delta E \sim 50$ at 6 keV, isolating individual regions with an accuracy ranging from $\sim$0.5″ (*Chandra*) to $\sim$5″(*XMM-Newton*). Before 1999 *ASCA* and *BeppoSAX* already provided imaging spectroscopy, but on arcminutes scales rather than arcseconds scales. The *Einstein* and *ROSAT* imagers on the other hand, had imaging resolution of $\sim$5″, but without any appreciable spectral resolution.

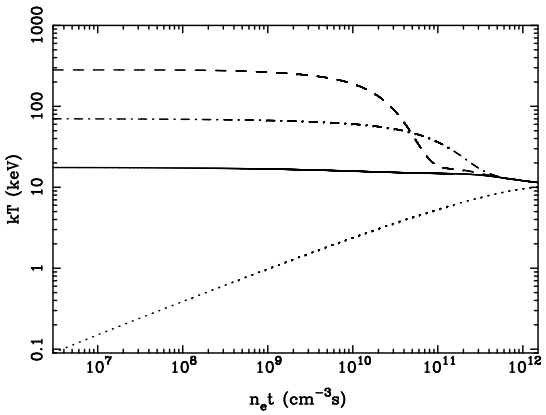

Figure 1. An illustration of the effect of temperature non-equilibration at the shock front. Shown is the temperature of electrons (dotted), protons (solid), helium (dashed-dotted) and oxygen ions (dashed) as a function of $n_{\rm e}t$, assuming that heating at the shock front is givenby Eq. 1. The oxygen-proton equilibration is faster than the helium-proton equilibration, as the cross sections scale linearly with particle mass, but quadratically with charge (Zeldovich & Raizer 1966).

Chandra and *XMM-Newton* also have dispersive high resolution spectrometers on board, three transmission gratings for *Chandra*'s, and two Reflective Grating Spectrometers (RGSs) for *XMM-Newton*. Due to their dispersive nature, these instruments are not ideal for spectrometry of extended objects. Nevertheless, for objects of modest extent, $< 1\ '$, the RGS is still able to obtain spectra with a resolution of $\lambda/\Delta\lambda > 160$ at 20 Å.

So what have these instrumental advances brought us, as

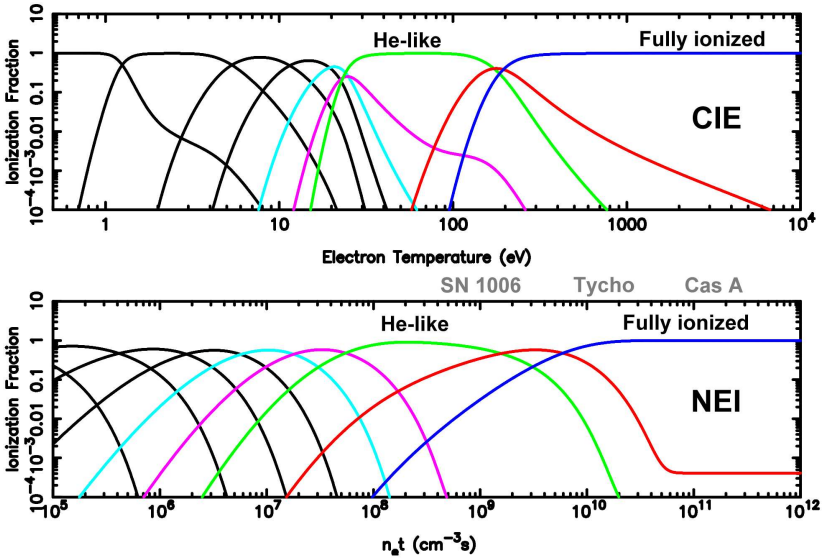

Figure 2. The effects of non-equilibration ionization (NEI) illustrated for oxygen. Both panels look very similar, but the top panel shows the oxygen ionization fraction as a function of electron temperature *for collisional ionization equilibrium (CIE), whereas the bottom panel shows the ionization fraction as function of $n_{\rm e}t$, and for a fixed temperature of $kT_{\rm e}$= 1.5 keV (based on Shull & van Steenberg 1982). Approximate, mean $n_{\rm e}t$ values for the plasma in the SNRs Cas A, Tycho and SN1006 are indicated.*

far as our knowledge of SNRs is concerned? The answer is that we have learned substantially about SNR shocks, concerning both the shock heating process and cosmic ray acceleration. Moreover, imaging spectroscopy has also revealed regions with metal-rich, pure ejecta plasma, and has provided us with better means to measure SNR kinematics through X-ray proper motion and Doppler shift studies.

Another important aspect is the study of supernova explosion through the analysis of kinematics of fresh explosive nucleosynthesis products. Finally, the high spatial resolution of in particular *Chandra* has enabled the discovery of many young neutron stars inside SNRs, such as the still enigmatic point source in Cas A that was discovered in the first light image of *Chandra* (Tananbaum 1999) (see also R. Petre these proceedings). However, in these proceedings I limit myself to three important topics 1) collisionless shock physics, 2) cosmic ray acceleration, and 3) supernova explosions and nucleosynthesis,

2. COLLISIONLESS SHOCKS PHYSICS

2.1. Background theory

SNR shocks typically move through a medium with densities of $n \sim 1$ cm^{-3}. At those low densities Coulomb (particle-particle) interactions are rare, with typical collision times given by $1/\tau = 8.8 \times 10^{-2}/T^{3/2} \ln \Lambda$ (Zeldovich & Raizer 1966). For temperatures of $T = 10^8$ K this gives $\tau \sim 12000$ yr ($\ln \Lambda$, the Coulomb is ~ 30). This is must longer than ages of many known SNRs. Nevertheless, we detect X-rays from young SNRs, which indicates that the plasma got heated despite the long collision times. This implies that the heating process takes place through long range collective effects, i.e. the generation of plasma waves. This is somewhat analogues to the process of violent relaxation in the formation of gravitational systems, such as galaxies and globular clusters.

The fact that supernova remnant shocks are collisionless and are also sites of cosmic ray acceleration has two important consequences. First of all, we can no longer assume that different particles species are in temperature equilibration. The amount of shock heating as a function of shock speed is obtained by applying energy, momentum and mass conservation to the gas crossing the shock front (e.g. McKee & Hollenbach 1980). In the extreme case in which particles of different mass do not interact, the temperature of each plasma component i (i.e. electrons, protons, other ions) is:

$$kT_i = \frac{2(\gamma-1)}{(\gamma+1)^2} m_i v_s^2 = \frac{3}{16} m_i v_s^2, \qquad (1)$$

where γ is the adiabatic index, m_i, is the particle mass, and v_s is the shock velocity. For full equilibration this is $kT = 3/16 < m > v_s^2$. In case full equilibration is not established at the shock front, Coulomb interactions will eventually establish equilibration on a collisional time scales, which is best characterized by the product of electron density and time $n_{\rm e}t$ (Fig. 1).

Secondly, Eq. 1 assumes that cosmic ray acceleration by the shock is energetically not important. In case the shock also accelerates an appreciable amount of cosmic rays, the mean plasma temperature may well be lower, a situation that may have been observed in the supernova remnant 0102.2-7219 (Hughes et al. 2000b).

When measuring the plasma temperatures by means of X-ray spectroscopy, one usually measures only the *electron* temperature, as it determines the shape of the bremsstrahlung continuum and it governs line intensity ratios. However, because the electron temperature can be lower than the average plasma temperature, it is wrong to infer a shock velocity from measured electron temperatures. This has been known for quite some time (e.g. Itoh

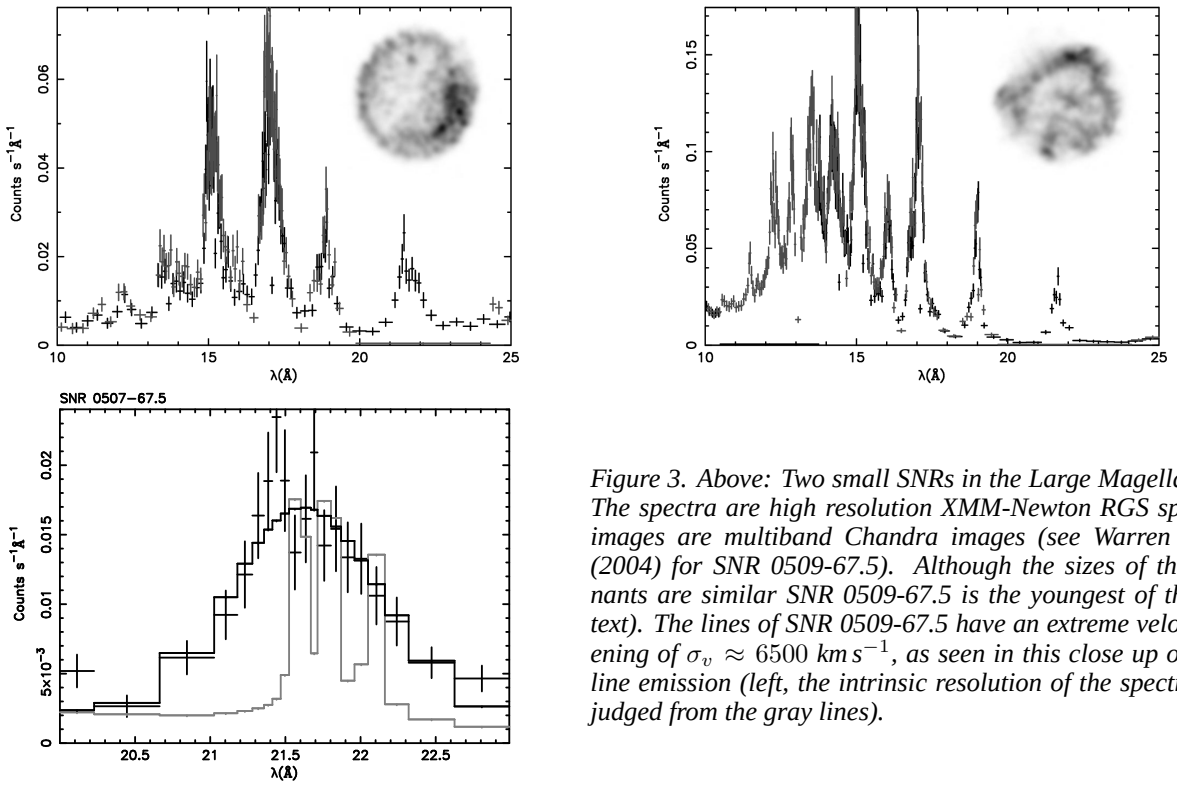

Figure 3. Above: Two small SNRs in the Large Magellanic Cloud. The spectra are high resolution XMM-Newton RGS spectra. The images are multiband Chandra images (see Warren & Hughes (2004) for SNR 0509-67.5). Although the sizes of the two remnants are similar SNR 0509-67.5 is the youngest of the two (see text). The lines of SNR 0509-67.5 have an extreme velocity broadening of $\sigma_v \approx 6500$ km s^{-1}, as seen in this close up of the O VII line emission (left, the intrinsic resolution of the spectrum can be judged from the gray lines).

1977, 1984), but until recently it was ignored, as it was difficult to assess the amount of temperature equilibration from the observational data.

Another form of non-equilibration, namely non-equilibration of ionization (NEI), has received more attention over the last two decades, because its signatures could be easily discerned in X-ray spectra of SNRs (e.g Winkler et al. 1981; Gronenschild & Mewe 1982; Jansen et al. 1988).

The concept of NEI is relatively simple (Itoh 1977; Mewe & Schrijver 1980; Liedahl 1999). NEI is important in SNRs, because in plasma that have been relatively recently heated the number of electron-ion collisions has been limited. Collisional ionization equilibrium (CIE) is obtained when the number of ionizations is compensated by the number of recombinations, but for NEI plasmas in SNRs the number ionization rates still exceed the recombination rate. The effect of NEI is illustrated in Fig. 2. Observationally NEI gives rise to a mismatch between the electron temperature derived from ratios of line emission from different ions, and the electron temperature derived from the continuum shape, which reflects the actual electron temperature. In addition, spectra of NEI plasmas will display lines that are unique for NEI, and are the result of inner shell excitations and ionizations (e.g. Vink 2004a, see).

2.2. High resolution spectra of supernova remnants

Although the effects of NEI were already known and observed in the eighties, the *XMM-Newton* RGS instruments make it possible to study it in much more detail. For extended objects the spectra are blurred due to the spatial extent of the objects, but the dispersion angle of the RGS is relatively large, allowing for high resolution spectroscopy of objects that are smaller than 1 $'$.[1] Even for larger objects, up to 5$'$, one can still obtain useful results with the RGS, especially at long wavelength, as has been done for the SNRs Cas A (Bleeker et al. 2001), Tycho (Decourchelle et al. 2001), and G292.0+1.8 (Vink et al. 2004).

However, the most detailed spectra are obtained for the various bright remnants in the Magellanic Clouds (Rasmussen et al. 2001; Behar et al. 2001; van der Heyden et al. 2002, 2003; van der Heyden et al. 2004).

Here I illustrate the capabilities of the RGS by showing two spectra of the Large Magellanic Cloud remnants 0509-67.5 and 0519-69.0. Both remnants have very similar sizes, resp. 29$''$ and 32$''$, but X-ray spectroscopy reveals, which one is the youngest of the two (Fig. 3). The spectra are dominated by O VII and O VIII line emission around 18.5 Å and 22 Å and Fe-L shell line emission, but for 0509-67.5 the Fe-L line emission shows mainly Fe emission at 15.0 and 17.1 Å, which reveals that the emission comes from Fe XVII (Ne-like Fe).

[1] For an angular extent of $\Delta\phi$ the degradation in spectral resolution is $\Delta\lambda \approx 0.12\Delta\phi$

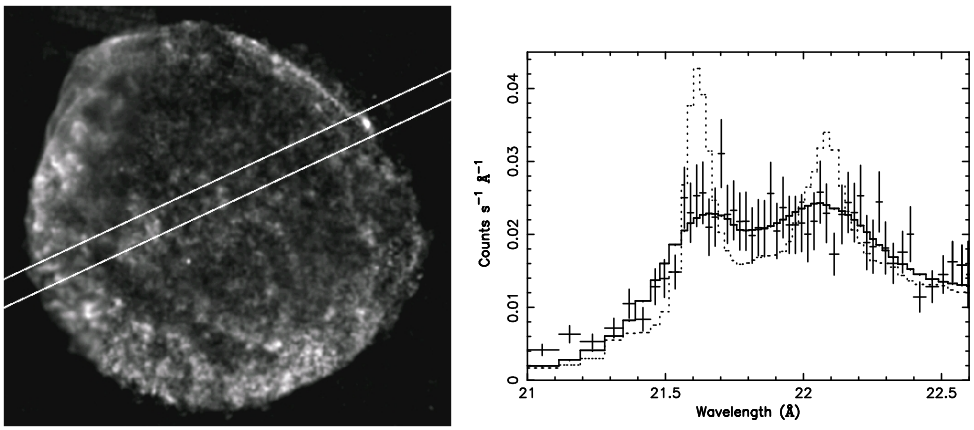

Figure 4. On the left: Map of O VII emission made from several Chandra-ACIS observations. The lines indicate the region observed by the XMM-Newton RGS instrument. The target was the bright knot in the northeast. Right: Detail of the RGS1 spectrum of the northeastern knot, showing O VII Heα line emission. The dashed line is the best fit model without line broadening, whereas the solid line shows the model including thermal line broadening (Vink et al. 2003).

SNR 0519-69.0 on the other hand shows also prominent emission lines at 12.0 Å, 13.5 Å, and 14.0 Å, an indication that Fe has been ionized up to Fe XXI. This shows that, despite the similarities in size, SNR 0519-69.0 is in a more evolved state. Spectral fitting indicates that $\log n_{\rm e}t \sim 10.1$ for 0509-67.5, and ~ 10.4 for 0519-69.0. More evidence that 0509-67.5 is younger comes from the line widths. Fig. 3 readily shows that the lines of 0509-67.5 are much broader than those of 0519-69.0. This is not a result of the spatial extent of the remnants, because SNR 0509-67.5 is the smallest of the two. The lines must therefore be broadened by Doppler broadening. For 0509-67.5 the O VIII Ly-α indicates a Gaussian broadening on top of the spatial broadening of $\sigma_v = 6500\pm$ km s^{-1}. For 0519-69.0 this is $\sigma_v = 1700 \pm 100$ km s^{-1}. Using the angular size of the remnants, and the distance to the Large Magellanic Cloud is 50 kpc, one obtains rough age estimates of respectively ~ 500 yr and ~ 2000 yr, assuming free expansion. For 0519-69.0 free expansion is probably unlikely, using instead the radius-velocity relation self-similar Sedov solution for a point explosion, $v_s = \frac{2}{5} r_s/t$, one finds ~ 800 yr.

2.3. An X-ray observation of non-equilibration of temperatures

Was non-equilibrium ionization a concept known and accepted by X-ray astronomers, non-equilibration of temperatures was sometimes mentioned as an annoying complication for interpreting data of SNRs, but for the most time it was simply ignored. Nevertheless, there were indications that non-equilibration is likely to be important. For example Eq. 1 predicts plasma temperatures of $kT \sim 30$ keV for shocks velocities of ~ 5000 km s^{-1}, applicable to young remnants such as Cas A, Tycho and SN1006. However, no SNR has ever been observed with temperatures exceeding even 5 keV.

Since 1995, however, more direct measurement of ion temperatures have indicated the importance of non-equilibration of temperatures. These measurements rely on the thermal Doppler broadening to measure the ion temperature. This has been done in the optical (Ghavamian et al. 2001, 2003), UV (Raymond et al. 1995; Laming et al. 1996; Korreck et al. 2004), and X-rays (Vink et al. 2003). The optical measurements use the fact that a fraction of the cold neutral hydrogen undergoes charge exchange with shock heated protons behind the shock. This results in Doppler broadened Hα emission.

The first X-ray measurement of the ion temperature was made with the *XMM-Newton*-RGS. It may be surprising that the target was a rather extended object: SN1006. This SNR has an extent of 30′. There were, however, two reasons to pick SN1006. First of all the X-ray spectrum shows that it is very far out of ionization equilibrium $\log n_{\rm e}t = 9.5$. Secondly, in order to isolate the thermal broadening from bulk motion from the expanding shell one has to isolate the edge of the remnant. This cannot be done with small remnants such as those in the Magellanic Clouds. For example, for SNR 0509-67.5 the line broadening is likely to be dominated by the shell expansion. For a large remnant such as SN1006 one can more easily isolate the outer edge. What made a high resolution X-ray spectrum possible despite the large extent of SN1006, was the fact that at the northeastern edge of the remnant there is a bright knot with a size of less than 1 ′(Fig. 4). Nevertheless, the RGS X-ray spectrum of the knot is contaminated by emission from the inside of SN1006. Luckily the northern part of SN1006 is not very bright, and the X-ray emission from the southern part is attenuated by the vignetting of the X-ray telescope.

The resulting RGS spectrum of SN1006 consists of lines that have a sharp rise at the short wavelength side, and a line wing at the long wavelength side, caused by X-ray emission from the inside of the remnant. Fig. 4 displays

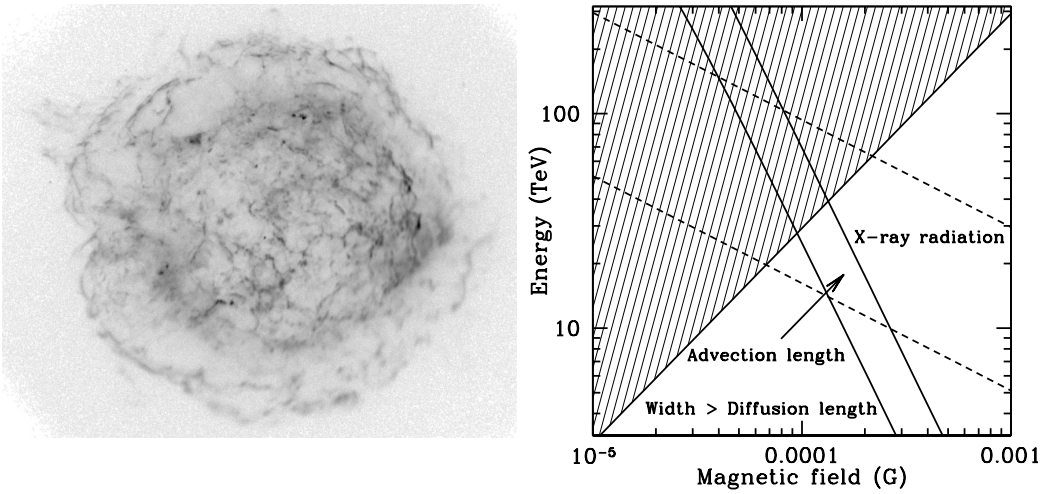

Figure 5. A deep Chandra image of Cas A (Hwang et al. 2004) in the 4-6 keV continuum band (left). Note the thin filaments, marking the border of the remnant (NB the point spread function is not uniform). The remnant has a radius of about 2.5′. Right: Determination of the maximum electron energy versus magnetic field strength for the region just downstream of Cas A's shock front, as determined from the thickness of the filaments. The shaded area is excluded, because the filament width cannot be smaller than the minumum possible diffusion length (c.f. Vink & Laming 2003).

the O VII Heα line triplet spectrum of this knot as observed by the RGS1. The spectrum can only be satisfactorily fitted with lines broadened with a Gaussian distribution with $\sigma_E = 3.4 \pm 0.5$ eV, corresponding to an oxygen temperature of ~ 500 keV (Vink et al. 2003). This seems to be a very high temperature, but it is in fact what can be expected for shock velocities of ~ 4000 km s^{-1} in the absence of rapid temperature equilibration (Eq. 1).

M. Markevitch showed at this symposium that the concept of non-equilibration of temperatures is also considered for shocks in clusters of galaxies. Contrary to SN1006, the Mach number $M \sim 3$ shock in the cluster 1E0657-56 is best explained by rapid equilibration of electron and ion temperatures. Together with SNR results this may contain important information about the physical conditions that determine the presence or absence of rapid equilibration:

For supernova remnants it has been observed that the fast shocks of young supernova remnants such as SN1006 and Tycho appear to have non-equilibrated plasma's, whereas the slow moving shocks of the Cygnus Loop (~ 300 km s^{-1}) seems to have rapidly equilibrated shocks. SNRs like Dem L71 and RCW 86 seem to have intermediate equilibration properties (Rakowski et al. 2003). It is not a priori clear what the physics is behind the different behavior of fast and slow shocks: Is the defining parameter shock speed, Mach number, or Alfven Mach number? The observation that the fast shock in 1E0657-56 does seem to equilibrate rapidly suggests that it is not the shock velocity as such, which is ~ 4500 km s^{-1} for 1E0657-56 (Markevitch et al. 2004). Instead it suggest that either the Mach number, or the Alfven Mach number is important for the equilibration process.[2]

[2]The Mach number is low in this case because the sound speed is very high.

3. COSMIC RAY ACCELERATION BY SUPERNOVA REMNANTS

Cosmic rays have been discovered by Victor Hess in 1912 (Hess 1912), but the question of their origin has still not been satisfactorily answered. SNRs are the most likely candidate sources for the origin of cosmic ray energies below 10^{15} eV, where there is a break in the spectrum, usually referred to as the "knee". It is clear that SNRs can provide the energy to maintain the cosmic ray energy density in the Galaxy. However, it was for a long time very doubtful that SNRs were capable of accelerating particles up to the "knee" (Lagage & Cesarsky 1983), let alone up to 10^{18} eV, at which energies the Galaxy becomes "transparent" to cosmic rays, and hence, at which energies there must be a transition from a Galactic origin to an extra-Galactic origin.

The last five years our understanding of cosmic ray acceleration by SNRs has changed dramatically, largely due to new theoretical insights, the coming of age of ground based TeV gamma-ray astronomy, and last but not least *Chandra*.

Cosmic rays are accelerated in supernova remnant shocks by the first order Fermi process (Malkov & O'C Drury 2001, for a review): Particles are accelerated by repeatedly diffusing across the shock, at each shock crossing the particles gains energy due to the difference in velocity at either side of the shock. For a high Mach number interstellar shock the compression ratio is 4, from which follows that the heated plasma behind the shock moves away from the shock with a velocity $v = 1/4 v_s$, with v_s the shock velocity. The difference in velocity between the unshocked and shocked medium is therefore $\Delta v = 3/4 v_s$.

SNR	Dist kpc	V_s km s^{-1}	n_0 cm^{-3}	width $''$	B_{loss} μG	B_{diff} μG
Cas A	3.4	5200	3	0.5	249	299
Kepler	4.8	5300	0.35	1.5	97	113
Tycho	2.4	4500	0.3	2	113	165
SN1006	2.2	4300	0.1	20	30	39
RCW86	2.5	3500	0.1	45	24	14

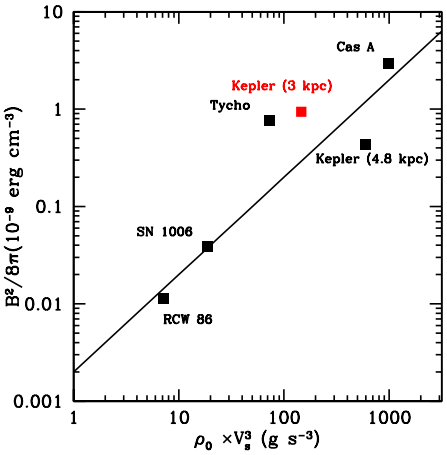

Figure 6. Left: Table with magnetic field determinations for various young supernova remnants (c.f. Bamba et al. 2005; Völk et al. 2005; Ballet 2005). Right: Magnetic field energy density as a function of ρV_s^3, following the suggestion by (Bell 2004). Note that in most cases velocities are based on radio and X-ray expansion measurements (Moffett et al. 1993; Vink et al. 1998; Hughes 1999, 2000; Delaney & Rudnick 2003), which introduces a systematic uncertainty for Kepler, for which no reliable distance estimate exists. Due to the narrow range in V_s and large range in densities, the scaling of B^2 with ρ is more significant than the scaling with v^3. (Vink et al. 2006, in preparation).

The diffusion process itself is a result of elastic scattering off magnetic field irregularities. The fastest possible diffusion, and hence the most efficient cosmic ray acceleration, is possible when $\delta B/B \sim 1$, and is referred to has Bohm-diffusion.

The cosmic ray population is dominated by ions, but in X-rays one can only observe the electron population by means of synchrotron radiation. X-ray synchrotron radiation from a shell type SNR is itself a recent discovery (Koyama et al. 1995). The contribution of *Chandra* is that it resolved for the first time narrow synchrotron filaments near the shock fronts of all young Galactic SNRs, such as Cas A and Tycho (Gotthelf et al. 2001; Hwang et al. 2002).

The width of these filaments can be interpreted as the result of advection combined with synchrotron losses: at TeV energies electron radiation losses are rapid. While diffusing in the downstream plasma, particles are on average moving away from the shock front with a velocity Δv. However, after a time τ_{loss} they are no longer visible in X-rays, because they have lost a significant fraction of their energy. Hence the observed width must correspond to $l_{adv} = \Delta v\, \tau_{loss}$ (Vink & Laming 2003). This in itself makes the width a function of Δv, particle energy, E, and average magnetic field, B, since $\tau_{loss} = 635/B^2 E$. In order to separate energy from magnetic field one can use the observed photon energy ϵ, which depends on E and B as $\epsilon = 7.4 E^2 B_\perp$ keV. In Fig. 5 shows graphically what the allowed range of electron energy and magnetic field is for Cas A: $B \approx 250 - 500$ μG (Vink & Laming 2003; Berezhko & Völk 2004). This is much higher than the shock compress mean Galactic magnetic field. In fact, it turns out that applying this method to all young SNRs gives relatively high magnetic fields (Bamba et al. 2005; Völk et al. 2005; Ballet 2005).

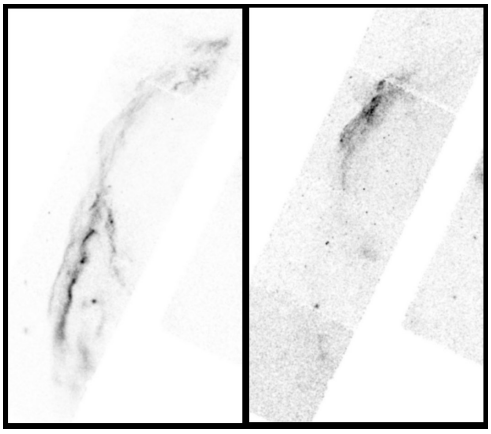

Figure 7. Two Chandra-ACIS images of the northeastern region of RCW 86. The left panel shows the energy range from 0.5-1.0 keV,which is dominated by thermal emission, whereas the right panel covers the range of 1.9-6.6 keV, dominated by synchrotron emission. (Vink et al. in preparation, see also Vink 2004b)

These higher magnetics confirm the hypothesis of Bell and Lucek that cosmic ray acceleration gives rise to magnetic field amplification due to non-linear plasma wave generation (Bell & Lucek 2001; Bell 2004). This in turns helps to speed up the cosmic ray acceleration process.

The magnetic field determinations of different studies differ in that some (Vink & Laming 2003) have employed the advection length l_{adv}, while others (Bamba et al. 2005; Völk et al. 2005) have used diffusion length scale,

l_{diff}. The diffusion length gives the typical length at which diffusive particle transport dominates over convection. The diffusion length scale is given by $l_{diff} = D/\Delta v = \frac{1}{3}c\lambda/\Delta v$, with D the diffusion coefficient, and λ the particle mean free path. For the fastest possible diffusion, Bohm diffusion, $\lambda = E/eB$. Bamba et al. (2005) and Völk et al. (2005) assumed Bohm diffusion in order to estimate magnetic field strengths. This is not a priori correct. However, the observed filament widths must at least be larger than the l_{diff} for Bohm diffusion. In fact when we take this additional constraint into consideration, we find that the results are consistent with the advection length method (Fig 5 and 6).

This is not entirely surprising (Vink 2004b): According to shock acceleration theory the acceleration time to reach an energy E, is given by $\tau_{acc} \approx D/(\Delta v)^2$.[3] For acceleration we need $\tau_{acc} \leq \tau_{loss}$. However, given that $l_{diff} = D/\Delta v$ and $l_{adv} = \Delta v\ \tau_{loss}$, we see that $\tau_{acc} \leq \tau_{loss}$ is equivalent with $l_{diff} \leq l_{adv}$. So whenever $l_{diff} \approx l_{adv}$ acceleration stops and the two length scales should give approximately the same answer. However, this is only the case at the very end of the electron cosmic ray spectrum, where synchrotron losses are important. This is consistent with X-ray observations, which show steep, loss affected, synchrotron spectra.

Moreover, the fact that the diffusion length method *assuming Bohm diffusion* is consistent with the advection length method implies that Bohm diffusion does indeed take place (see also Markowith, these proceedings, for more details). This also means that SNRs are more efficient cosmic ray accelerators than previously thought for two reasons: 1) fast diffusion applies and 2) magnetic fields are amplified. In fact assuming Bohm diffusion Cas A must be able to accelerate particles up to energies of $\sim 2 \times 10^{15}$ eV for protons and $\sim 10^{17}$ eV for iron. Moreover, the magnetic field amplification is predicted by Bell (2004) to scale roughly as $B^2 \propto \rho V_s^3$, which seems indeed to be the case (Fig. 6). This means that the highest energy cosmic rays may by those shocks that are fast and have a high density. These conditions are met by remnants of supernovae with red supergiant progenitors. These progenitors have a slow and therefore dense wind. Moreover, the shock velocity remains high for a long period due to the $1/r^2$ density profile. In fact, Cas A's progenitor was probably a red supergiant (Vink 2004).

4. EXPLOSIVE NUCLEOSYNTHESIS

Over the last few years the study of supernovae have become more popular for two reasons: One concerns Type Ia supernovae, which are likely thermonuclear explosions of white dwarfs. These supernovae have with great success been used as standard candles in cosmology, which has led to the revival of the cosmological constant. The other reason is that long duration gamma-ray bursts (GRBs) appear to be associated with special subclass of core collapse supernovae called Type Ib/c supernovae (e.g. Stanek et al. 2003).

It is not always possible to associate SNRs with the various types of supernovae. However, it is clear that all SNRs with an associated neutron star must be core-collapse supernovae. Thanks to *Chandra* it is now also clear that a number of young SNRs in the LMC are likely to be Type Ia SNRs. In all those cases the SNRs show an increase in Fe abundance toward the center. This is exactly what should be expected as Type Ia supernovae are thought to produce ~ 0.5 M$_\odot$ of ^{56}Ni (which decays into Fe), much more than the average core collapse supernovae.

It is interesting to use existing SNRs to illustrate the evolutionary sequence of Type Ia remnants, showing that while the reverse shock progresses inward into the ejecta, more and more of Fe gets heated (see Badenes et al. 2005, for more sophisticated description of Type Ia remnant evolution). One could start with 0509-67.5 (Fig. 3 Warren & Hughes 2004), in which the reverse shock seems to have just reached the Fe layer in the east. The next one would be 0519-69.0 (Fig. 3) or alternatively Tycho's SNR (Hwang & Gotthelf 1997; Hwang et al. 2002), in which more Fe seems to be shocked, in a shell all around the remnant. The final stage is represented by DEM L71 (Hughes et al. 2003; van der Heyden et al. 2003), for which all of ~ 0.5 M$_\odot$ of Fe appears to be shocked by the reverse shock. In DEM L71 the Fe is no longer in shell, but seems to fill the whole center of the remnant.

A peculiar case seems to SN1006. The historical supernova is likely to have been a Type Ia explosion, but both optical/UV absorption (Wu et al. 1997), and in X-ray emission (Vink et al. 2000, 2003; Vink 2004a) there seems to be a lack of Fe. For the X-ray emission the reason could be that the reverse shock has not yet reached the Fe-layer. Moreover, the plasma is so far out of ionization equilibrium (Sect. 2.1) that even if Fe is shocked heated it will still have an ionization state lower than Fe XVII, producing hardly any emission lines.

The evolution of remnants of core collapse supernovae are not so easily illustrated by a sequence of SNRs. For one thing, the presence of a powerful pulsar wind nebula does in some cases completely dominate the appearance of a SNR. Moreover, the lack of a well defined sequence may very well reflect the variety of core collapse progenitors, which is also the reason why they are unsuitable as standard candles. Core collapse explosions seem also more turbulent than Type Ia explosions, so that the initial ordering of stellar layers is not preserved during the explosion. The best evidence for that consists of the early appearance of ^{56}Co radio-active line emission from SN1987A (observations are summarized in Vink 2005), and the presence of Fe-rich ejecta *outside* the main, Si-rich, shell in the southeast of Cas A (Hughes et al. 2000a; Hwang & Laming 2003). In the north the Fe is located

[3] I have ignored here some small numerical factor that reflect the fact that the particles spend time on both sides of the shock front, and at each side the magnetic field is different due to magnetic field compression

inside the Si-rich shell. However, this appears to be a projection effect, because the measured Doppler velocities of Fe in the north is higher than Si (Willingale et al. 2002). It is not clear how much of the Fe in Cas A is still unshocked, but some of the shocked Fe must have been ejected with velocities of up to 7800 km s^{-1}.

There is no obvious symmetry to the Fe-rich ejecta, so their emergence is probably related to hydrodynamical instabilities close to the core of the explosion (Kifonidis et al. 2003). Cas A does, however, reveal an intriguing symmetry when dividing the X-ray map of Si XIII emission by that of Mg XI emission (Fig. 8). It does not only bring out the long known jet in the East, but also a counterpart symmetrical situated in the West of the remnant (Vink 2004; Hwang et al. 2004). The spectra of the jet reveal an apparent absence of Ne and Mg. The dominant elements seem to be Si, S, and Ar, but some Fe seems also present. The emission measure of the jet combined with the average velocity of the plasma suggest quite a high kinetic energy in the jet, $\sim 5 \times 10^{50}$ erg, about 25% of the total explosion energy.

The presence of a jet/counter jet system suggests a connection with long duration GRBs, which are thought to be the results of beamed emission from jets. In that case the jets in Cas A could be the result of a similar mechanism, although resulting in lower velocities than for GRB jets. However, the point source in Cas A seems to be neutron star, at odds with the currently popular collapsar theory for GRBs, for which the a core collapse into a black hole is needed(MacFadyen et al. 2001). Secondly, GRB jets are thought to be generated deep inside the star. One would therefore naively expect the jet material to be dominated by core material, i.e. Fe. Still, GRB jets may be electro-magnetic in nature. Moreover, for the few promising, but still disputed cases in which line emission from GRBs has been detected, there seems to be an absence of Fe or Ni emission (e.g. Watson et al. 2003). Note in this context that Cas A has long been thought to be the remnant of a Type Ib explosion, the same subclass that seems to produce GRBs.

Further exploration of the 1 million second *Chandra* observation of Cas A (Hwang et al. 2004) may reveal more about the nature of its jet/counter jet system. Moreover, Cas A is one of two SNRs that is known to contain detectable amounts of the radio-active element ^{44}Ti (Iyudin et al. 1994; Vink et al. 2001). This element is synthesized deep inside the exploding star, in the same layer as ^{56}Ni, but the ^{44}Ti yield is very sensitive to the explosion energy and asymmetries. The observation of ^{44}Ti in Cas A is therefore very important for studying its explosion properties. This is one of the reasons for observing Cas A with INTEGRAL, the first results of which are promising, but have allowed us to obtain conclusion regarding the kinematics of ^{44}Ti (Fig. 9, Vink 2005). Nevertheless, this is an important goal, since ^{44}Ti emission comes both from the shocked and unshocked parts of the ejecta.

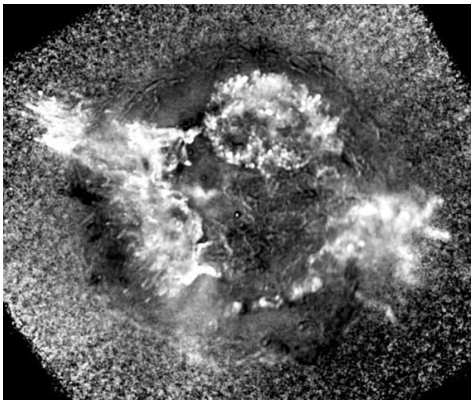

Figure 8. Image based on the deep Chandra observation of Cas A, which has been processed to bring out the jet/counter jet structure (Vink 2004; Hwang et al. 2004). (Credit: NASA/CXC/GSFC/U.Hwang et al.)

5. CONCLUDING REMARKS

An overview like this is not much more than summing up the conclusions of many individual studies. So what can I add to that, except reiterating that the successful launch of *Chandra* and *XMM-Newton* has given us many new insights into the shock heating, cosmic ray acceleration, and composition of SNRs. Many old questions seem to have been (partially) answered, such as the question of electron-ion temperature equilibration at the shock front (electron-ion equilibration is not efficient in fast shocks), or the question whether cosmic rays can be accelerated up to the "knee" by supernova remnant shocks (yes they can). New questions have been raised by the new observational capabilities, such as the nature of the jet/counter jet system in Cas A.

In that respect the investigation of SNRs is very similar to other topics discussed at this meeting. So let me therefore conclude by thanking the organizers for having invited me to this very interesting and stimulating meeting.

REFERENCES

Badenes, C., Borkowski, K. J., & Bravo, E. 2005, ApJ, 624, 198
Ballet, J. 2005, ArXiv Astrophysics e-prints
Bamba, A., Yamazaki, R., Yoshida, T., Terasawa, T., & Koyama, K. 2005, ApJ, 621, 793
Behar, E., Rasmussen, A. P., Griffiths, R. G., et al. 2001, A&A, 365, L242
Bell, A. R. 2004, MNRAS, 353, 550
Bell, A. R. & Lucek, S. G. 2001, MNRAS, 321, 433
Berezhko, E. G. & Völk, H. J. 2004, A&A, 419, L27
Bleeker, J. A. M. et al. 2001, A&A, 365, L225
Decourchelle, A. et al. 2001, A&A, 365, L218
Delaney, T. & Rudnick, L. 2003, ApJ, 589, 818

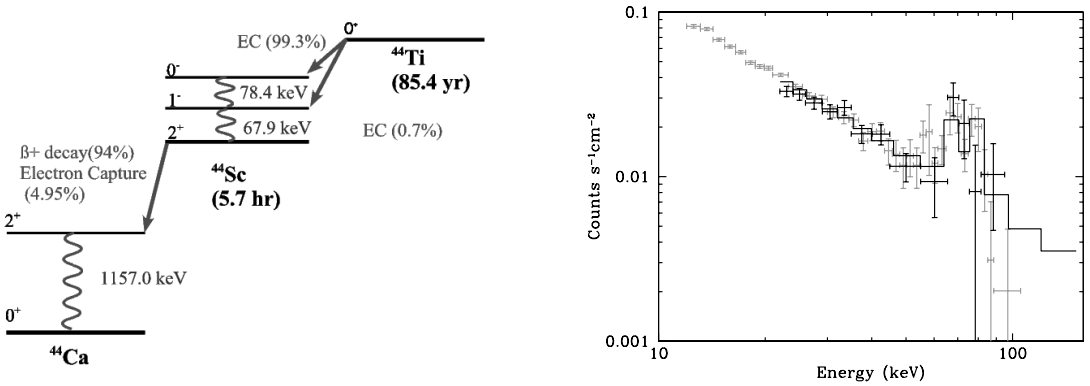

Figure 9. Left: The radio active decay scheme of ^{44}Ti. Right: hard X-ray spectrum, as observed by BeppoSAX (in gray) and INTEGRAL, both showing clear signs of emission around 68 keV and 78 keV due to ^{44}Ti decay lines (Vink 2005).

Ghavamian, P., Rakowski, C. E., Hughes, J. P., & Williams, T. B. 2003, ApJ, 590, 833
Ghavamian, P., Raymond, J., Smith, R. C., & Hartigan, P. 2001, ApJ, 547, 995
Gotthelf, E. V. et al. 2001, ApJ, 552, L39
Gronenschild, E. & Mewe, R. 1982, A&AS, 48, 305
Hess, V. F. 1912, Physik. Zeitschr., 13, 1084
Hughes, J. P. 1999, ApJ, 527, 298
Hughes, J. P. 2000, ApJ, 545, L53
Hughes, J. P., Ghavamian, P., Rakowski, C. E., & Slane, P. O. 2003, ApJ, 582, L95
Hughes, J. P., Rakowski, C. E., Burrows, D. N., & Slane, P. O. 2000a, ApJ, 528, L109
Hughes, J. P., Rakowski, C. E., & Decourchelle, A. 2000b, ApJ, 543, L61
Hwang, U., Decourchelle, A., Holt, S. S., & Petre, R. 2002, ApJ, 581, 1101
Hwang, U. & Gotthelf, E. V. 1997, ApJ, 475, 665
Hwang, U. & Laming, J. M. 2003, ApJ, 597, 362
Hwang, U. et al. 2004, ApJ, 000, 000
Itoh, H. 1977, PASJ, 29, 813
Itoh, H. 1984, ApJ, 285, 601
Iyudin, A. F. et al. 1994, A&A, 284, L1
Jansen, F. et al. 1988, ApJ, 331, 949
Kifonidis, K., Plewa, T., Janka, H.-T., & Müller, E. 2003, A&A, 408, 621
Korreck, K. E., Raymond, J. C., Zurbuchen, T. H., & Ghavamian, P. 2004, ApJ, 615, 280
Koyama, K. et al. 1995, Nature, 378, 255
Lagage, P. O. & Cesarsky, C. J. 1983, A&A, 125, 249
Laming, J. M., Raymond, J. C., McLaughlin, B. M., & Blair, W. P. 1996, ApJ, 472, 267
Liedahl, D. A. 1999, Lecture Notes in Physics, Berlin Springer Verlag, 520, 189
MacFadyen, A. I., Woosley, S. E., & Heger, A. 2001, ApJ, 550, 410
Malkov, M. A. & O'C Drury, L. 2001, Reports of Progress in Physics, 64, 429
Markevitch, M., Gonzalez, A. H., Clowe, D., et al. 2004, ApJ, 606, 819
McKee, C. F. & Hollenbach, D. J. 1980, ARA&A, 18, 219
Mewe, R. & Schrijver, J. 1980, A&A, 87, 261
Moffett, D. A., Goss, W. M., & Reynolds, S. P. 1993, AJ, 106, 1566
Rakowski, C. E., Ghavamian, P., & Hughes, J. P. 2003, ApJ, 590, 846
Rasmussen, A. P. et al. 2001, A&A, 365, L231
Raymond, J. C., Blair, W. P., & Long, K. S. 1995, ApJ, 454, L31
Shull, J. M. & van Steenberg, M. 1982, ApJS, 48, 95
Stanek, K. Z. et al. 2003, ApJ, 591, L17
Tananbaum, H. 1999, IAU Circ., 7246, 1
Völk, H. J., Berezhko, E. G., & Ksenofontov, L. T. 2005, A&A, 433, 229
van der Heyden, K. J., Bleeker, J. A. M., & Kaastra, J. S. 2004, astro-ph/0309030 (A&A accepted)
van der Heyden, K. J., Bleeker, J. A. M., Kaastra, J. S., & Vink, J. 2003, A&A, 406, 141
van der Heyden, K. J. et al. 2002, A&A, 392, 955
Vink, J. 2004a, astro-ph/0412447
Vink, J. 2004, astro-ph/0409517
Vink, J. 2004b, New Astronomy Review, 48, 61
Vink, J. 2005, *Adv. Space Res.*, 35, 976
Vink, J., Bleeker, J., Kaastra, J. S., & Rasmussen, A. 2004, Nucl. Phys. B Proc. Suppl., 132, 62
Vink, J., Bloemen, H., Kaastra, J. S., & Bleeker, J. A. M. 1998, A&A, 339, 201
Vink, J., Kaastra, J. S., Bleeker, J. A. M., & Preite-Martinez, A. 2000, A&A, 354, 931
Vink, J. & Laming, J. M. 2003, ApJ, 584, 758
Vink, J., Laming, J. M., Gu, M. F., Rasmussen, A., & Kaastra, J. 2003, ApJ, 587, 31
Vink, J. et al. 2001, ApJ, 560, L79
Warren, J. S. & Hughes, J. P. 2004, ApJ, 608, 261
Watson, D., Reeves, J. N., Hjorth, J., Jakobsson, P., & Pedersen, K. 2003, ApJ, 595, L29
Willingale, R., Bleeker, J. A. M., van der Heyden, K. J., Kaastra, J. S., & Vink, J. 2002, A&A, 381, 1039
Winkler, P. F., Clark, G. W., Markert, T. H., Petre, R., & Canizares, C. R. 1981, ApJ, 245, 574
Wu, C., Crenshaw, D. M., Hamilton, A. J. S., et al. 1997, ApJ, 477, L53+
Zeldovich, Y. & Raizer, Y. P. 1966, Elements of gasdynamics and the classical theory of shock waves (New York: Academic Press, 1966, edited by Hayes, W.D.; Probstein, Ronald F.)